Advanced Materials Design Group amdg.science

Vascular Transpiration in a Carbon-Carbon Composite Leading Edge

Olima M, Latheef MA, LePage W, Ramsurn H, Keller MW

PUBLISHED AS

Olima M, Latheef MA, LePage W, Ramsurn H, Keller MW. “Vascular Transpiration in a Carbon-Carbon Composite Leading Edge.” AIAA AVIATION 2026 Forum (2026).

https://doi.org/10.2514/6.2026-4436

Copyright © 2026 by the American Institute of Aeronautics and Astronautics, Inc. This is the accepted version; the Version of Record is available at https://doi.org/10.2514/6.2026-4436.

Self-archived by the authors in accordance with the publisher’s self-archiving policy. Provided for educational and personal use. Please cite the version of record.

ACCEPTED MANUSCRIPT · SELF-ARCHIVED AUTHOR VERSION

Vascular Transpiration in a Carbon-Carbon Composite Leading Edge

Mark H. Olima *, Mohammed Ammar Abdul Latheef †, William LePage ‡, Hema Ramsurn §, and Michael W. Keller ¶
The University of Tulsa, Tulsa, OK, 74104

Carbon-carbon (C/C) composites are among the few structural materials capable of surviving the aerothermal environment of hypersonic flight, yet integrating active cooling into a monolithic C/C leading edge without thermal expansion mismatch, assembly complexity and flow impingement has not previously been demonstrated. Heat pipe embedded C/C structures are constrained by coefficient of thermal expansion mismatch, while porous transpiration-cooled designs exhibit poor coolant outflow at the stagnation point, which is the region of highest heat flux. This paper presents the fabrication of a 2D laminate C/C composite leading edge incorporating integrated vascular coolant channels and engineered interconnected porosity within a 3 mm shell for dual mode active cooling. The 0.4 mm diameter vascular channels were formed using a Vaporization of Sacrificial Component (VaSC) approach and survived densification cycle without blockage. Schlieren imaging under argon flow at 1000 psi supply pressure on a representative piece demonstrated a continuous coherent surface film, with a steady 400 psi outlet pressure confirming sustained transpiration through the porous matrix.

Nomenclature

CTE	=	coefficient of thermal expansion
PLA	=	polylactic acid
I-CVI	=	isothermal chemical vapor infiltration

I. Introduction

Aerodynamic heating presents a fundamental challenge for hypersonic flight. At high Mach numbers, kinetic energy is converted to thermal energy and transferred through the vehicle surface into the structure, with leading-edge temperatures reaching up to 2000°C at Mach 10 for a given leading-edge radius [1]. These extreme

*Graduate Student, Department of Mechanical Engineering, 430 S Gary Place, and Student Member AIAA.
†Graduate Student, Russell School of Chemical Engineering, 430 S Gary Place.
‡Assistant Professor, Department of Mechanical Engineering, 430 S Gary Place.
§Associate Professor, Russell School of Chemical Engineering, 430 S Gary Place.
¶Associate Dean for Research, Department of Mechanical Engineering, 430 S Gary Place.

temperatures constrain both the attainable velocity and the operational duration of hypersonic vehicles given current material technology. Thermal protection systems (TPS), including passive, semi-passive, and active approaches have been extensively documented for hypersonic applications [2]. Among semi-passive approaches, heat pipe structures have been embedded in carbon-carbon (C/C) composites using refractory metals such as molybdenum, tungsten, and tantalum. Tenney et al. [3] demonstrated the successful embedding of tungsten tubes within 2D C/C composites using lithium as a working fluid, while Glass et al. [4] fabricated and tested a C/C composite leading edge at 1000°C incorporating molybdenum-rhenium heat pipes. However, processing complications and coefficient of thermal expansion (CTE) mismatch between embedded pipes and the surrounding composite matrix impose an effective temperature ceiling on these approaches, limiting their suitability for vehicles that must endure very high heating rates, high enthalpy flow, and elevated stagnation pressures.

Active transpiration cooling has been proposed as a means of overcoming these limitations [5], with coolant injected through a porous surface to form a protective film and reduce net heat flux at the wall. Characterizing suitable porous materials and understanding outflow behavior at hypersonic conditions have been the focus of extensive experimental and numerical investigation in recent years [6]. Ifti et al. [7] fabricated and tested a porous zirconium diboride panel at Mach 7, demonstrating that helium achieves greater heat flux reduction than nitrogen at equivalent blowing ratios owing to superior thermophysical properties and higher volumetric flow rate. Numerical work by Luo et al. [8] on a double-layer transpiration-cooled leading edge confirmed that low-density coolants generate recirculation at the stagnation zone that displaces the high-temperature region, but that uniform porous media remain limited by permeability anisotropy. Shen et al. [9] experimentally confirmed that cooling effectiveness is consistently lowest at the stagnation point under high aerodynamic heating and elevated stagnation pressure, regardless of coolant type. The geometry of the porous medium itself presents a further challenge: Dittert et al. [10] characterized the surface outflow of a porous C/C composite cone with an internal plenum and observed negligible mass flux at the tip, the region of highest thermal loading, attributing this to permeability anisotropy from fiber orientation. These ground-based findings were echoed in the first hypersonic flight experiment on transpiration-cooled sharp fins, reported by Di Martino et al. [11], in which shock wave impingement locally blocked coolant effusion at the leading edge of C/C-SiC fins, yielding non-uniform cooling efficiency. A practical manufacturing route to achieve controllable, uniform active cooling across the full leading edge, including the stagnation region, in a monolithic C/C structure has not yet been demonstrated.

Here we present a novel C/C composite leading edge incorporating integrated vascular coolant channels and spatially engineered porosity, intended to address the outflow non-uniformity identified in prior work. By replacing discrete heat pipes and injectors with a monolithic vascular and porous architecture, the design is conceived to eliminate CTE mismatch and assembly complexity, while providing a dedicated internal cooling pathway at the tip and enabling controlled transpiration over the remainder of the surface. Realizing this architecture in a C/C composite presents significant processing challenges: the engineered porosity must remain open and interconnected throughout processing,

and the interface between the channel network and the surrounding porous matrix must be free of densification-induced blockage.

II. Methods

A C/C composite leading edge was fabricated with a process adapted from Cordiero et.al [12], with manual pre-form layup, depolymerization via Vaporization of Sacrificial Components (VaSC) for channel formation, carbonization via pyrolysis, densification and graphitization. The mandrel was machined from aluminum with a tip radius of 5 mm. The part presented here, with a 12-ply layup, (6 woven, 2 unidirectional and 6 woven), was fabricated with Mitsubishi K13C for the woven layers (640 W/m.K) and Mitsubishi K63712 (140 W/m.K) for the unidirectional layers. PLA filaments (0.4 mm diameter) were used as the sacrificial material to form channels during depolymerization. During the fiber layup, the top peel ply was perforated to ensure the gases evolved during autoclave processing (curing) are removed through vacuum, thereby reducing porosity from trapped gases and moisture (Fig.1).

The cross-section of the green body was examined using a Keyence VHX 1000 digital microscope. X-ray Computed Tomography (X-ray CT) was subsequently performed using a Zeiss Xradia Versa 620 to scan the leading edge after de-polymerization and verify the condition of the embedded channels.

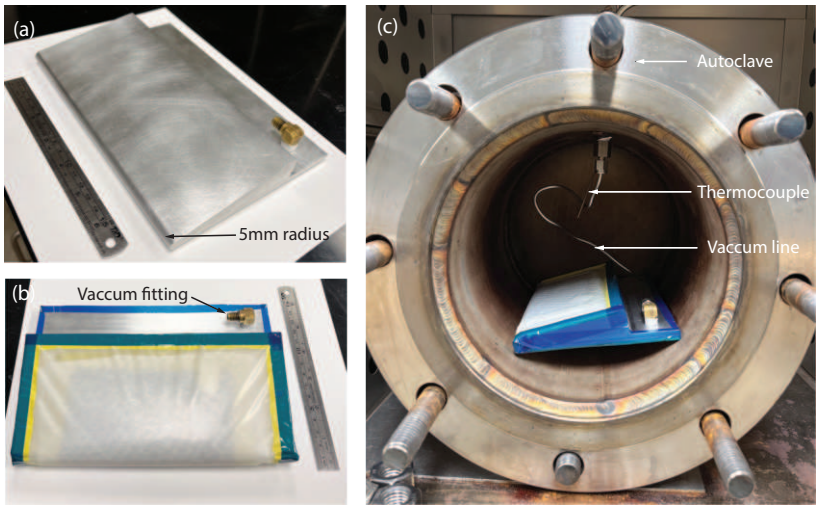

Fig. 1 Leading-edge (a) aluminum mold (b) vacuum bagged prepreg and (c) autoclave setup.

To characterize the transpiration capability of the vascular C/C composite, a representative piece was placed in a pressurization rig (Fig.2), capable of reaching up to 1000 psi. A pressure transducer on the inlet and outlet measured the differential pressure and the readings were recorded using an NI DAQ on a LabView program. Schlieren imaging is used to visualize the flow through the porous surface. A 114 mm diameter concave mirror with a 900 mm focal length is placed behind the sample, and a camera placed at a distance twice the focal length of the mirror with a light source next to it. The refractive index gradient between the flow emanating from the surface of the sample and the surrounding

ambient environment enables optical visualization of the flow field. As light reflects off the mirror and traverses the flow region, variations in refractive index alter the light path through refraction. These deviations are captured by the camera, allowing for detailed imaging of the flow structure as shown in Fig.2.

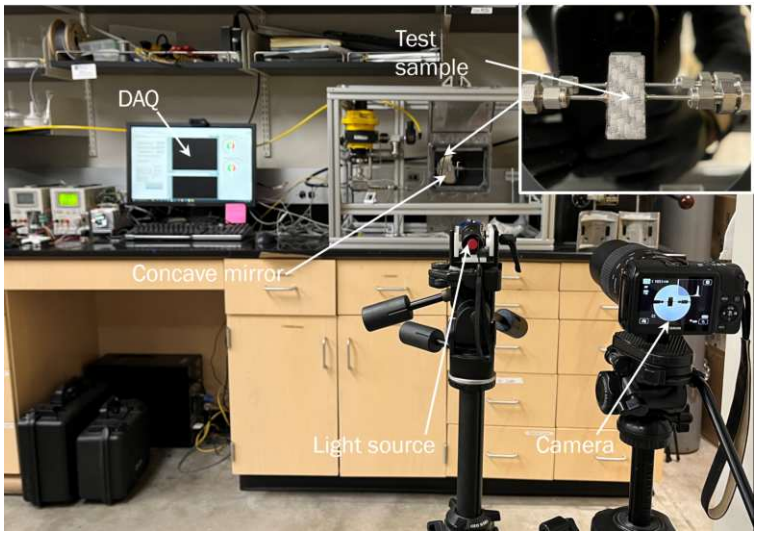

Fig. 2 Dual Schlieren imaging pressurization rig.

III. Results and Discussion

After removal from the autoclave, the pre-preg retained the mold's shape (Fig.3 a-b). The part was then heated at 250°C under vacuum overnight to depolymerize the PLA and leave clear channels in the pre-preg (Fig.3 c-d). Argon gas was flown through the channels to ensure that the channels were unclogged (Fig.3 e).

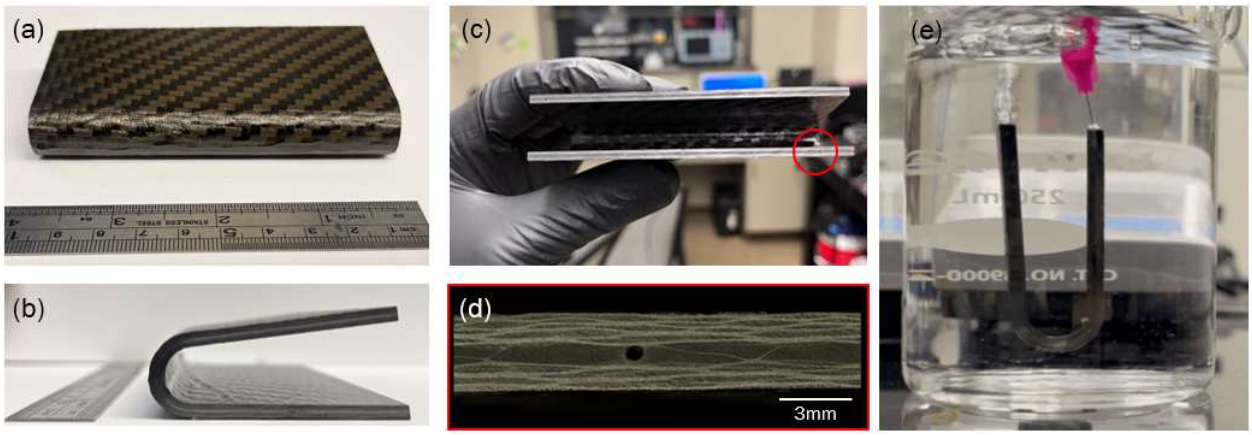

Fig. 3 Green part with (a) smooth surface finish (b) near net leading-edge shape (c-d) round channels and (e) clear channels.

X-ray CT scans of the nose (Fig.4 b), upper (Fig.4 c) and lower surfaces (Fig.4 d) of the green body corroborate the argon flow test results, confirming the presence of continuous, well-defined, and unobstructed channels.

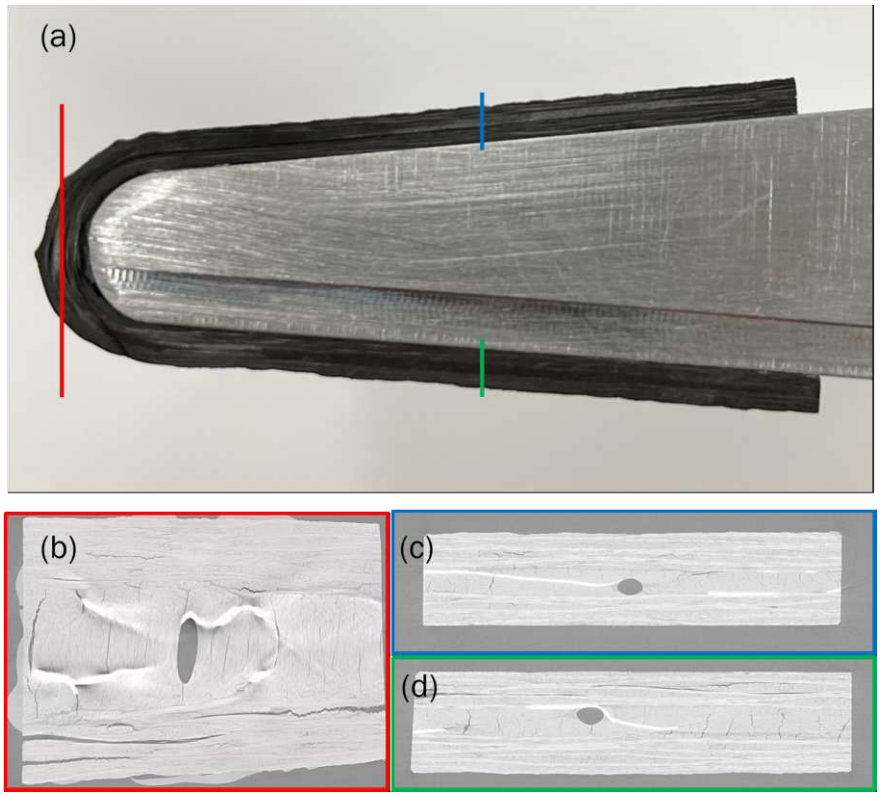

Fig. 4 (a) Cross section of leading edge post-depolymerization and XCT image of (b) nose, (c) upper-surface and (d) lower-surface sections.

The green part was then carbonized at 1000°C in an inert environment with the channel openings still maintaining their shape (Fig.5 a-b). Argon was flown through a channel of a sectioned piece that was dipped in water: bubbles could be seen forming on the surface confirming that the part was still porous with some of the Argon gas also passing through the channel to the other opening, confirming a clear path (Fig.5 c-d).

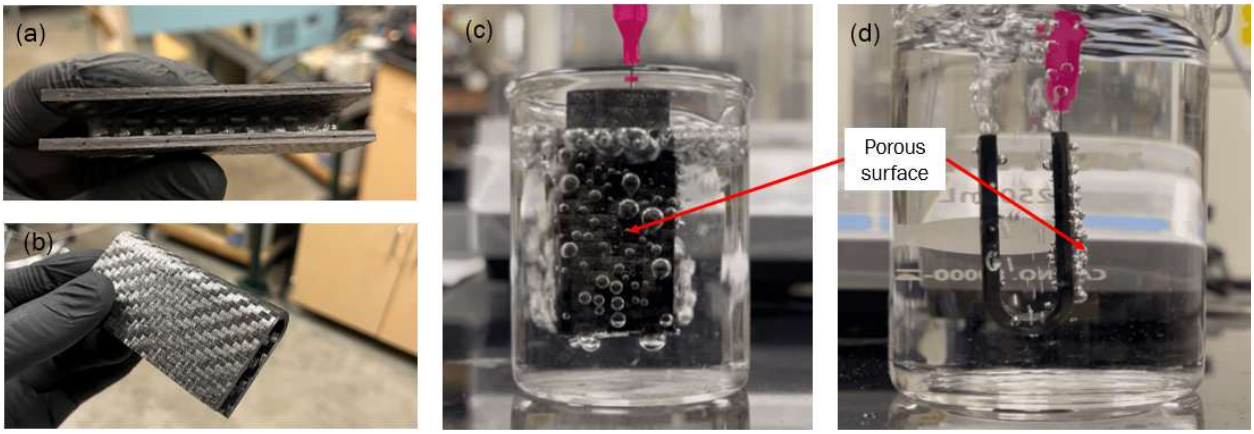

Fig. 5 Carbonized C/C composite leading edge (a) with clear channels (b) good surface finish (c) porous surface and (d) showing argon gas passing to the surface and through a channel.

A cross-section of the green body, examined using a digital microscope, revealed localized resin-starved regions from autoclave compaction over the curved geometry (Fig.6 b). After subsequent carbonization, the part had voids and matrix shrinkage cracks from mass loss and volatilization associated with pyrolysis [13–16]. Notably, the pitch fibers, which exhibit high stiffness, remained intact and unbroken across the curvature from a 5 mm inner radius to a 8 mm outer radius (Fig.6 c).

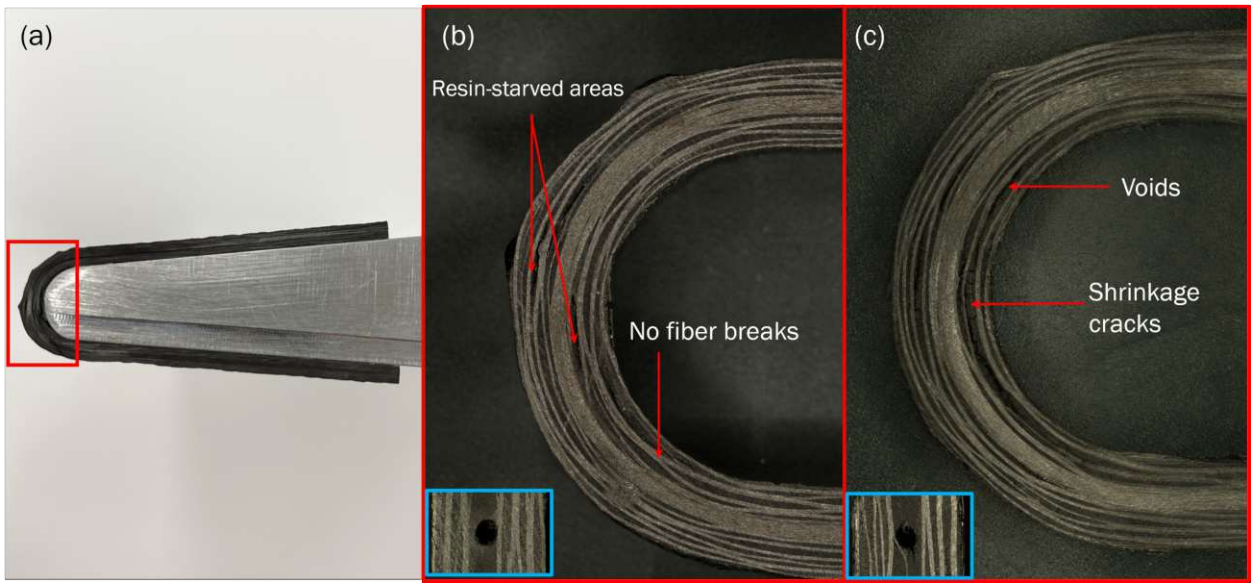

Fig. 6 Cross section of (a) leading edge (b) post-depolymerization and (c) post-carbonization.

After carbonization, the part underwent a 20-hour I-CVI densification cycle using methane as a precursor. Argon was again flown through the channel, confirming that the paths remained unobstructed. During the pressurization test, at a pressure of 1000 psi, an argon gas jet was observed emanating from the representative vascular C/C composite sample using Schlieren imaging (Fig.7) confirming the transpiration nature of the sample. The transducer at the inlet read 578.35 ± 2.27 psi and the outlet transducer read 508 ± 1.22 psi, Fig.8,confirming a steady performance for over 135 seconds.

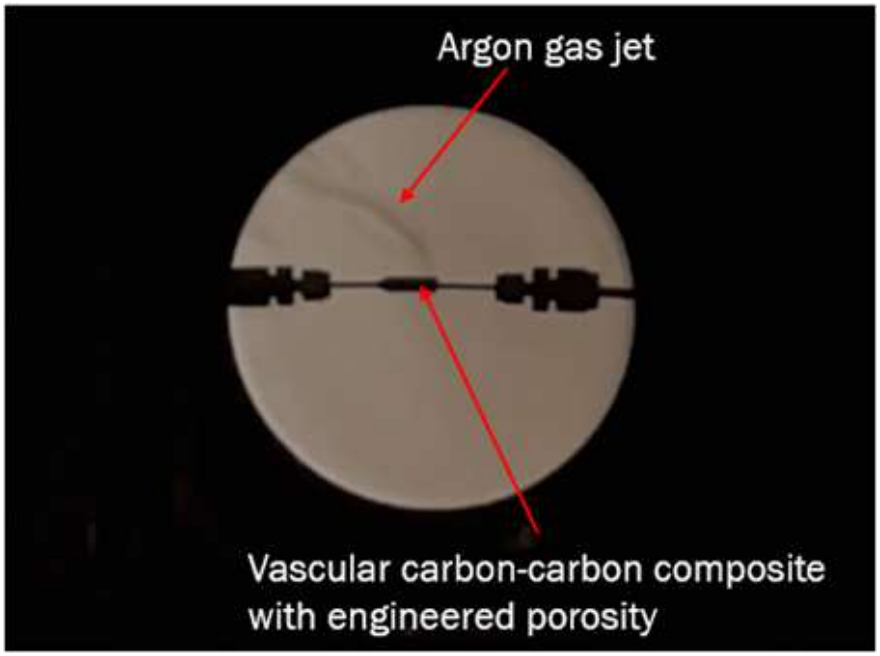

Fig. 7 Schlieren imaging showing transpiration nature of vascular C/C composite after an input of 1000 psi.

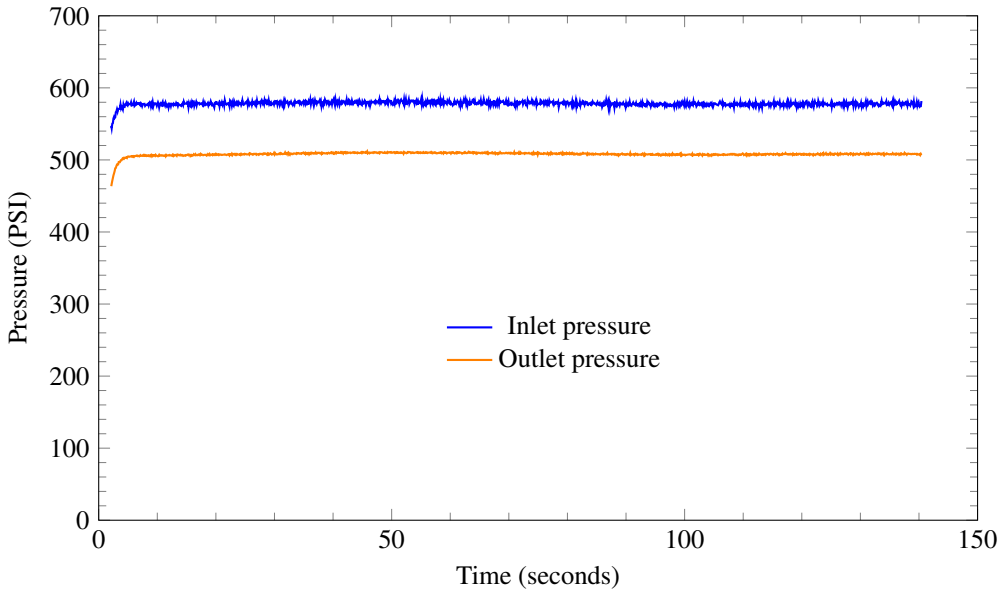

Fig. 8 Vascular C/C composite coupon inlet and outlet pressure .

IV. Conclusions

The stagnation-point cooling limitations of existing porous transpiration designs, combined with the processing and CTE constraints of heat pipe embedded C/C structures, motivated the development of a monolithic actively cooled C/C leading edge. XCT imaging confirmed that the 0.4 mm vascular channels formed by the VaSC method survived

processing. Schlieren imaging on a representative piece demonstrated the formation of a continuous coherent surface film under argon flow at 1000 psi supply pressure, with a sustained outlet pressure of around 500 psi for 135 seconds confirming active transpiration through the porous matrix. These results establish that the proposed architecture is both geometrically intact and maintains continuous pathways following processing, representing a manufacturable solution to the assembly complexity, thermal expansion incompatibility and stagnation-point flow impingement that constrain prior designs. Aerothermal performance characterization of the leading edge under representative hypersonic heating conditions will be the subject of a subsequent publication.

Acknowledgments

This research was supported by Department of Energy, Office of Science under award number DE-SC0024402 and Department of Defense, Air Force Office of Scientific Research under award number FA9550-24-1-0212. Special thanks to Philip Noel for assisting with XCT imaging.

References

[1] Ohlhorst, C. W., Glass, D. E., Bruce, W., Lindell, M., Vaughn, W. L., Smith, R., Dirling, R. B., Hogenson, P. A., Nichols, J. M., Risner, N., Thompson, D. R., Kowbel, W., Sullivan, B. J., Koenig, J. R., and Cuneo, J. C., "Development of X-43A Mach 10 Leading Edges," *56th International Astronautical Congress of the International Astronautical Federation, the International Academy of Astronautics, and the International Institute of Space Law*, American Institute of Aeronautics and Astronautics, Fukuoka, Japan, 2005. https://doi.org/10.2514/6.IAC-05-D2.5.06, URL https://arc.aiaa.org/doi/10.2514/6.IAC-05-D2.5.06.

[2] Glass, D., "Ceramic Matrix Composite (CMC) Thermal Protection Systems (TPS) and Hot Structures for Hypersonic Vehicles," *15th AIAA International Space Planes and Hypersonic Systems and Technologies Conference*, American Institute of Aeronautics and Astronautics, Dayton, Ohio, 2008. https://doi.org/10.2514/6.2008-2682, URL https://arc.aiaa.org/doi/10.2514/6.2008-2682.

[3] Tenney, D. R., Lisagor, W. B., and Dixon, S. C., "Materials and structures for hypersonic vehicles," *Journal of Aircraft*, Vol. 26, No. 11, 1989, pp. 953–970. https://doi.org/10.2514/3.45868, URL https://arc.aiaa.org/doi/10.2514/3.45868.

[4] Glass, D. E., Camarda, C. J., Merrigan, M. A., and Sena, J. T., "Fabrication and Testing of Mo-Re Heat Pipes Embedded in Carbon/Carbon," *Journal of Spacecraft and Rockets*, Vol. 36, No. 1, 1999, pp. 79–86. https://doi.org/10.2514/2.3436, URL https://arc.aiaa.org/doi/10.2514/2.3436.

[5] Henline, W. D., "Transpiration Cooling of 1 : Hypersonic Blunt Bodies with Finite Rate Surface Reactions," 1989.

[6] Böhrk, H., Piol, O., and Kuhn, M., "Heat Balance of a Transpiration-Cooled Heat Shield," *Journal of Thermophysics and Heat Transfer*, Vol. 24, No. 3, 2010, pp. 581–588. https://doi.org/10.2514/1.47172, URL https://arc.aiaa.org/doi/10.2514/1.47172.

[7] Ifti, H. S., Hermann, T., Ewenz Rocher, M., Doherty, L., Hambidge, C., McGilvray, M., and Vandeperre, L., "Laminar

transpiration cooling experiments in hypersonic flow," *Experiments in Fluids*, Vol. 63, No. 6, 2022, p. 102. https://doi.org/10.1007/s00348-022-03446-1, URL https://doi.org/10.1007/s00348-022-03446-1.

[8] Luo, S., Miao, Z., Liu, J., Song, J., Xi, W., and Liu, C., "Effects of Coolants of Double Layer Transpiration Cooling System in the Leading Edge of a Hypersonic Vehicle," *Frontiers in Energy Research*, Vol. 9, 2021. https://doi.org/10.3389/fenrg.2021.756820, URL https://www.frontiersin.org/journals/energy-research/articles/10.3389/fenrg.2021.756820/full.

[9] Shen, L., Wang, J., Dong, W., Pu, J., Peng, J., Qu, D., and Chen, L., "An experimental investigation on transpiration cooling with phase change under supersonic condition," *Applied Thermal Engineering*, Vol. 105, 2016, pp. 549–556. https://doi.org/10.1016/j.applthermaleng.2016.03.039, URL https://www.sciencedirect.com/science/article/pii/S1359431116303313.

[10] Dittert, C., Selzer, M., and Böhrk, H., "Flowfield and Pressure Decay Analysis of Porous Cones," *AIAA Journal*, Vol. 55, No. 3, 2017, pp. 874–882. https://doi.org/10.2514/1.J055298, URL https://arc.aiaa.org/doi/10.2514/1.J055298.

[11] Di Martino, G. D., Peichl, J., Hufgard, F., Duernhofer, C., Loehle, S., and Göser, J., "Main flight data on transpiration cooled sharp edge fins in hypersonic conditions on the sounding rocket HIFLIER," *Aerospace Science and Technology*, Vol. 158, 2025, p. 109895. https://doi.org/10.1016/j.ast.2024.109895, URL https://www.sciencedirect.com/science/article/pii/S1270963824010241.

[12] Cordeiro, J. C., Zuzelski, M., Olima, M. H., Crunkleton, D. W., Otanicar, T., Ramsurn, H., and Keller, M. W., "Vascular Carbon/Carbon composites for concentrated solar power," *Composites Part A: Applied Science and Manufacturing*, Vol. 180, 2024, p. 108069. https://doi.org/https://doi.org/10.1016/j.compositesa.2024.108069, URL https://www.sciencedirect.com/science/article/pii/S1359835X24000666.

[13] Schulte-Fischedick, J., Zern, A., Mayer, J., Rühle, M., and Voggenreiter, H., "The crack evolution on the atomistic scale during the pyrolysis of carbon fibre reinforced plastics to carbon/carbon composites," *Composites Part A: Applied Science and Manufacturing*, Vol. 38, No. 10, 2007, pp. 2237–2244.

[14] Lavaggi, T., Muhammed, F., Moretti, L., Gillespie Jr, J. W., and Advani, S. G., "Correlation of the permeability and porosity development of carbon/carbon composites during pyrolysis," *Composites Part A: Applied Science and Manufacturing*, Vol. 181, 2024, p. 108156.

[15] Ko, T.-H., Kuo, W.-S., and Chang, Y.-H., "Raman study of the microstructure changes of phenolic resin during pyrolysis," *Polymer composites*, Vol. 21, No. 5, 2000, pp. 745–750.

[16] Souza, W. O. d., Garcia, K., Von Dollinger, C. F. d. A., and Pardini, L. C., "Electrical behavior of carbon fiber/phenolic composite during pyrolysis," *Materials Research*, Vol. 18, No. 6, 2015, pp. 1209–1216.